AIP | Journal of Applied Physics

Rotational modes in a phononic crystal with fermion-like behavior

P. A. Deymier, K. Runge, N. Swinteck, and K. Muralidharan

Citation: Journal of Applied Physics **115**, 163510 (2014); doi: 10.1063/1.4872142
View online: http://dx.doi.org/10.1063/1.4872142
View Table of Contents: http://scitation.aip.org/content/aip/journal/jap/115/16?ver=pdfcov
Published by the AIP Publishing

Rotational modes in a phononic crystal with fermion-like behavior

P. A. Deymier, K. Runge, N. Swinteck, and K. Muralidharan
Department of Materials Science and Engineering, University of Arizona, Tucson, Arizona 85721, USA

(Received 10 February 2014; accepted 10 April 2014; published online 24 April 2014)

The calculated band structure of a two-dimensional phononic crystal composed of stiff polymer inclusions in a soft elastomer matrix is shown to support rotational modes. Numerical calculations of the displacement vector field demonstrate the existence of modes whereby the inclusions and the matrix regions between inclusions exhibit out of phase rotations but also in phase rotations. The observation of the in-phase rotational mode at low frequency is made possible by the very low transverse speed of sound of the elastomer matrix. A one-dimensional block-spring model is used to provide a physical interpretation of the rotational modes and of the origin of the rotational modes in the band structure. This model is analyzed within Dirac formalism. Solutions of the Dirac-like wave equation possess a spinor part and a spatio-temporal part. The spinor part of the wave function results from a coupling between the senses (positive or negative) of propagation of the wave. The wave-number dependent spinor-part of the wave function for two superposed waves can impose constraints on the integral of the spatio-temporal part that are reflected in a fermion-like lifting of degeneracy in the phonon band structure associated with in-phase rotations.
 [http://dx.doi.org/10.1063/1.4872142]

I. INTRODUCTION

Phononic crystals (PCs) comprised of periodically arranged elastic scatterers of one material dispersed periodically throughout a different homogeneous matrix material can strongly affect the propagation of acoustic and/or elastic waves.[1] Several studies have considered the role rigid body rotations may play in modifying the bulk modes of propagation in the phononic structure.[2–8] Sainidou *et al.*[5] and Zhao *et al.*[6] revealed theoretically that rotary resonance modes can strongly interact with Bragg gaps to yield extremely wide absolute acoustic band gaps. Peng *et al.*[8] proposed a one-dimensional lumped model composed of finite-sized masses and mass-less springs to provide an understanding of the underlying physics behind rotary resonance in two-dimensional (2D) solid/solid PCs. The notion of modeling a PC from a continuum perspective (with additional degrees of freedom, namely rotation) relates to the work done by the Cosserat brothers over one hundred years ago.[9] In 1909, the Cosserat brothers pioneered a continuum theory of elasticity that accounted for the rotational degrees of freedom of individual elements in addition to the standard translational degrees of freedom used in classical elasticity theory. In the Cosserat model, each material element has six degrees of freedom—three for translation and three for rotation. The theory introduces a couple-stress tensor (a component arising from the coupling of rotational and shear waves) that fulfills the same role for torques as the stress tensor of classical elasticity plays for forces. Ultimately, Cosserat continuum elasticity theory predicts that rotational degrees of freedom (e.g., rotational wave modes) can strongly modify the dispersion of shear waves.[10] Several studies have characterized rotational elastic waves in three-dimensional (3D) granular structures comprised of pre-compressed, regular arrangements of spherical elastic particles.[11–13] In these works, the Hertz-Mindlin contact model is used to represent the connection between the elements of the structure. The existence of transverse vibrations in the structures necessitates the consideration of rotation for the individual spherical particles. Rotational degrees of freedom in the structure showed individual rotational modes as well as coupled rotary/translational modes in the dispersion relations.[11,12]

It is known that Cosserat elasticity restricted to rotations only provides a framework for the alternative description of the electron.[14] It has also been shown that rotational waves in an isotropic continuous elastic solid can be described within the formalism of the Dirac equation providing a classical interpretation of relativistic quantum mechanics.[15] Conical Dirac dispersions or Dirac-like behavior in photonic crystals (the electromagnetic wave counterpart of PC)[16–19] and PC[20,21] have also recently received attention. Longhi[22] and Ref. 17 provide a derivation of the 1D Dirac's equation from the coupled modes equations of a lattice of waveguides in terms of two sublattices. In these optical waveguide sublattice models, the discrete couple mode equations form a set of two equations involving discrete finite differences. These finite discrete differences are transformed in the long wavelength limit into continuous derivatives to arrive at a continuous 1D Dirac equation, which solutions are two-component spinors. Longhi[23] also proposed a photonic analogue of the relativistic Dirac oscillator by considering the propagation of electromagnetic wave in continuous 1D Bragg gratings.

While phonons are bosons, the isomorphism between Cosserat media supporting rotational degrees of freedom and the Dirac formalism (relativistic wave equation representing spin $^1/_2$, fermion, particles[24]) suggests the possibility of characterizing rotational waves in PC within a fermion-like formalism.

Here, we report on the investigation of a 2D PC constituted of stiff polymer inclusions in a soft elastomer matrix.

The 2D PC composed of a square array of polystyrene (PS) inclusions in a polydimethylsiloxane (PDMS) elastomer matrix is shown to support rotational waves. Of particular interest are modes where the PS inclusions and the region of the matrix separated by the inclusions rotate out of phase but also in phase. Following Peng *et al.*,[8] who demonstrated that a 1D lumped mass model can be used to describe rotational modes in a 2D PC, we introduce a 1D mass spring phononic structure that can also support rotational waves. The 1D model is used to reproduce the dispersion relations of the 2D system in a certain range. The 1D model is further analyzed to provide a physical interpretation of the origin of the bands associated with rotational modes. For this, the classical wave equation for rotational waves in the 1D phononic structure is rewritten in the form of Dirac-like equations. The wave functions solutions of these equations take on spinor character associated with the sense of propagation of the wave (positive and negative frequency). The degeneracy or non-degeneracy of the band structure is related to constraints imposed by the spinor-part of the wave function on the integral of the spatio-temporal part of the wave function.

The paper is organized as follows. In Sec. II, we introduce a 2D PC composed of rod-like, stiff polymer inclusions of square cross-section embedded in a soft elastomer matrix. It is shown computationally that this PC exhibits a band structure that supports rotational waves. The rotational bands are identified by calculating the displacement vector field of individual modes. Two types of rotational modes are observed, namely modes that are characterized by out of phase but also in phase rotational motion in the inclusions and the matrix regions between inclusions. In Sec. III, we present a 1D harmonic phononic structure that can support rotational waves. It was shown that a 1D model can be used to reproduce some of the bands associated with rotational modes in 2D PC and provide an interpretation of their physical origin.[8] Here, we rewrite the rotational wave equation within Dirac formalism. In particular, we introduce an exact square root expression for the discrete Laplacian operator of the 1D model that leads to a Dirac-like equation involving 4x4 matrix operators. We consider several cases of rotational waves and obtain their corresponding wave functions in the form of the product of a spinor part (a four-spinor) and a spatio-temporal part. We then consider the superposition of two rotational waves and the constraint the spinor structure of the rotational wave functions imposes on the integral of the spatio-temporal part. This fermion-like behavior is related to the characteristics of the band structure of the 1D and subsequently 2D phononic structures and in particular to the band associated with the in-phase rotational mode. In Sec. IV, conclusions are drawn as to the observability of fermion-like behavior and implications for the development of future functionalities of PC.

II. TWO-DIMENSIONAL PHONONIC CRYSTALS SUPPORTING ROTATIONAL WAVES

A. Model and method

The PC of interest is composed of a square array of PS cylinders with square cross section embedded in a homogeneous, elastic matrix of PDMS. This combination of materials offers distinctive elastic band structures with modes corresponding to rotational waves. PS and PDMS are unique due to their sharp contrast in transverse speed of sound and low-density. The elastic parameters for PS and PDMS are as follows: $\rho_{PS} = 1050\,kg/m^3$, $C_{L,PS} = 2350\,m/s$, $C_{T,PS} = 1230\,m/s$, $\rho_{PDMS} = 965\,kg/m^3$, $C_{L,PDMS} = 1100\,m/s$, and $C_{T,PDMS} = 200\,m/s$, where ρ, C_L, and C_T denote density, longitudinal speed of sound, and transverse speed of sound, respectively. The lattice constant of the PC is $a = 1\,cm$. The length of the edge of the square inclusion is 0.6 cm for a filling fraction $ff = 0.36$ (see Figure 1(a) for schematic). The structural mechanics module of the commercial software package COMSOL Multiphysics is utilized to generate the phonon band structure of the PC and visualize displacement vector fields for specific Eigen modes.

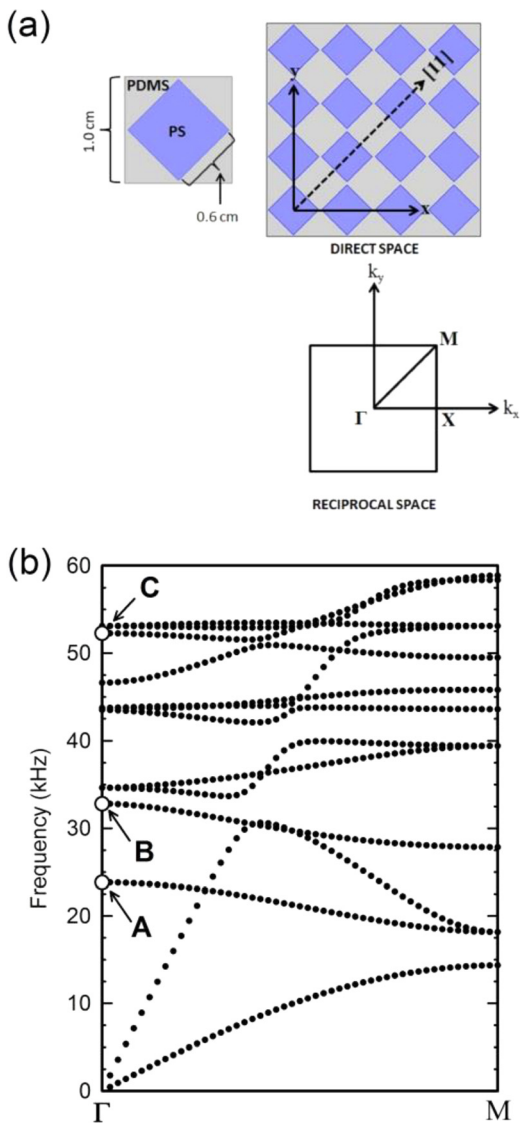

FIG. 1. (a) Schematic representation of the direct space and reciprocal space unit cells of the PC composed of a square lattice of PS inclusions (square cross-section) embedded in a PDMS matrix. (b) Phonon band structure (xy-modes) along ΓM-direction in reciprocal space.

B. Band structure and eigenmodes of the 2D phononic crystal

The dispersion diagram along the ΓM-direction in reciprocal space ([11]-direction in direct space) is shown in Figure 1(b). Longitudinal and transverse acoustic branches stem from the Γ-point in the dispersion diagram. These bands span the width of the 1st Brillouin zone and fold back into the zone at the boundary (M-point), thus yielding multiple longitudinal and shear optical branches. Several hybridization gaps are observable between the longitudinal acoustic branch and higher frequency optical modes possessing similar symmetry, several of which possess mixed translation and rotational character.

Our specific interest in Figure 1(b) is identifying rotational modes with pure rotational character. Modes "A," "B," and "C" in Figure 1(b) at the Γ-point possess this characteristic. We illuminate these Eigen modes in Figure 2 with finite-element calculations of displacement vector fields.

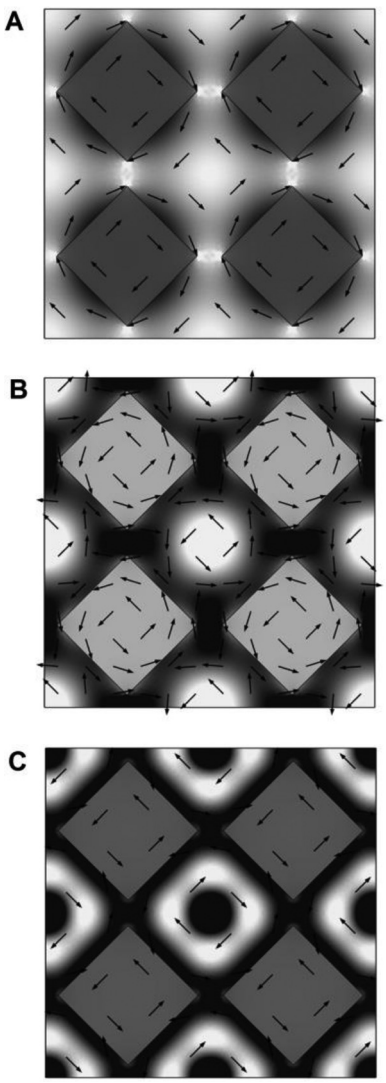

FIG. 2. Displacement vector field (arrows) of the PS/PDMS phononic crystal corresponding to Eigenmodes "A," "B," and "C" in Figure 2(b). The grey color-scale (not shown) corresponds to the z-component of the curl of the displacement field.

For mode A, along the [11]-direction, alternating regions of PS and PDMS exhibit out of phase rotations. This is also the case for mode C. Similar modes have been observed in a steel-epoxy solid/solid PC.[8] In contrast, the mode B shows that the PS and PDMS regions are rotating in phase. The observation of a well-defined in-phase rotational mode at low frequency is enabled by the very low value of the transverse speed of sound in the PDMS compared to that of the PS inclusions. Indeed, we have verified that increasing $C_{T,\,PDMS}$ results in a shift of the mode "B" toward higher frequencies where this mode will hybridize with other modes. To elucidate the origin of the two types of rotational modes observed in the 2D PC, we use a 1D Cosserat-like micromechanics model. It was demonstrated in Ref. 8 that such a 1D model can reproduce the dispersion relations associated with rotational modes in a 2D PC composed of a square array of solid inclusions in a solid matrix.

III. ONE-DIMENSIONAL DISCRETE COSSERAT-LIKE MICROMECHANICS MODEL

A. Model and method

Vassiliev *et al.*[25,26] have studied a discrete linear one-dimensional micromechanics model that includes longitudinal, shear, and rotational degrees of freedom. This 1D discrete Cosserat-like lattice model consists of an infinite chain of square block elements (Cosserat elements) connected with multiple harmonic springs. Each element in the model is considered to have two translational degrees of freedom (displacement in the x and y directions) and one rotational degree of freedom (rotation about an axis perpendicular to the xy-plane). Figures 3(a) and 3(b) show the repeatable unit cells for the monoblock and diblock Cosserat lattice models, respectively. Figure 3(a) shows periodicity (h) and Figure 3(b) shows periodicity ($2h$). The diblock system mimics the behavior of alternating extended regions of PS and PDMS connected via elastic springs.

Three different harmonic springs (spring constants k_0, k_1, and k_2) connect different parts of the Cosserat elements.

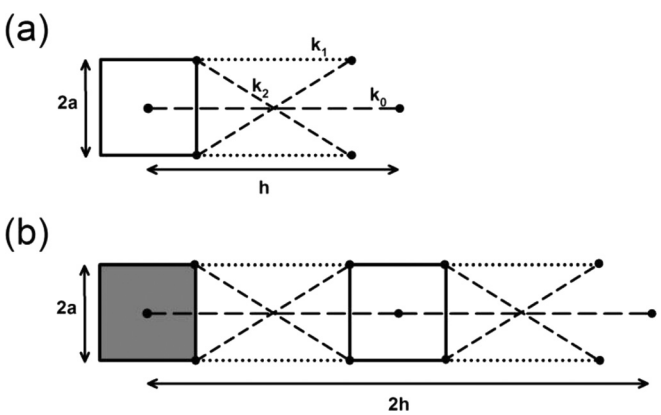

FIG. 3. Schematic illustration of the discrete Cosserat-like micromechanics model. (a) Unit cell of the monoblock model with Cosserat elements (blocks) connected by three types of harmonic springs (spring constants k_0, k_1, and k_2). Each Cosserat element possesses translational longitudinal (u), shear (v), and rotational (φ) degrees of freedom. (b) Unit cell of a diblock model.

The Cosserat element in Figure 3(a) has mass (m) and moment of inertia (I). The Cosserat elements that make-up the diblock unit cell have masses (m_1 and m_2) and inertial moments (I_1 and I_2). For Figure 3(a), the Cosserat element in the nth unit cell has x-displacement (u_n), y-displacement (v_n) and rotation component (φ_n). u_n and v_n represent displacements associated with longitudinal and transverse vibrations, respectively. The potential energy associated with the elastic connections of elements (n) and (n + 1) in the monoblock chain is written as follows:

$$E_{n,n+1} = \frac{1}{2}K_0(u_{n+1} - u_n)^2 + \frac{1}{2}K_1\left[(v_{n+1} - v_n) + \frac{h}{2}(\varphi_{n+1} + \varphi_n)\right]^2 + \frac{1}{2}K_2(\varphi_{n+1} - \varphi_n)^2, \quad (1)$$

where $K_0 = \left(\frac{k_0}{h^2} + \frac{2k_1}{l^2} + \frac{2k_2 l^2}{l_d^4}\right)$, $K_1 = \left(\frac{2k_2(2a)^2}{l_d^4}\right)$, $K_2 = \left(\frac{2a^2 k_1}{l^2}\right)$, $l = h - (2a)$, and $l_d = \sqrt{(l^2 + (2a)^2)}$. Accordingly, the equations of motion for the Cosserat element in the nth unit cell of the monoblock lattice are written as

$$m\frac{d^2u_n}{dt^2} = K_0(u_{n+1} - 2u_n + u_{n-1}), \quad (2)$$

$$m\frac{d^2v_n}{dt^2} = K_1(v_{n+1} - 2v_n + v_{n-1}) + \frac{hK_1}{2}(\varphi_{n+1} - \varphi_{n-1}), \quad (3)$$

$$I\frac{d^2\varphi_n}{dt^2} = K_2(\varphi_{n+1} - 2\varphi_n + \varphi_{n-1}) + \frac{hK_1}{2}(v_{n-1} - v_{n+1}) - \frac{h^2K_1}{4}(\varphi_{n+1} + 2\varphi_n + \varphi_{n-1}). \quad (4)$$

B. Band structure of the 1D micromechanics model

Utilizing Eqs. (1)–(4), we numerically generate phonon band structures for the monoblock and diblock systems by implementing the finite-difference scheme described in Ref. 27 for a similar 1D system. For the monoblock model, we chose m = 25 g, a = 0.35 cm, h = 1.414 cm, k_0 = 55 000 N·m, k_1 = 9500 N·m, and k_2 = 6500 N·m. The numerical values of these parameters are chosen to establish a semiquantitative correspondence between the band structure of the 1-D block systems and that of the 2-D PC. In particular, we obtain semiquantitative agreement in (a) the ordering of the bands (modes A, B, and C), (b) the symmetry of the modes as well as (c) the order of magnitude of the frequencies of these modes. The diblock system is identical to the monoblock system except for the mass (and consequently moment of inertia) of the Cosserat elements (m_1 = 27 g and m_2 = 23 g). Figures 4(a) and 4(b) shows the dispersion diagrams for the monoblock and diblock systems, respectively.

The band structure of the monoblock lattice contains three bands corresponding to the three degrees of freedom (u, v, and φ). The bands rendered with unfilled circles support modes with rotational character (as shown by Eqs. (3) and (4)) while the band comprised of solid circles corresponds to modes with translational character only (see Eq. (2)). The points marked by "A," "B," and "C" correspond to modes with pure rotational character. The band structure of the diblock system (Figure 4(b)) exhibits the characteristic band folding associated with the doubling of the period. We have retained on that figure the location of the monoblock rotational modes (eigenmodes "A," "B," and "C"). At the origin, the rotational mode marked by "B" is characterized by each block rotating in phase with its neighbor. Modes "A" and "C" correspond to rotational waves whereby alternating blocks rotate with a π phase shift. These modes are isomorphic to those observed in the more complex band structure of the 2D PC. We subsequently employ the 1D model to provide additional physical understanding of the rotational modes and in particular in-phase rotational modes. More specifically, we are interested in interpreting mode "B" with in-phase rotation of the PS and PDMS domains. Since the nature of mode "B" is the same for the monoblock and diblock systems, we investigate it in the case of a simplified monoblock model using the formalism of Dirac.

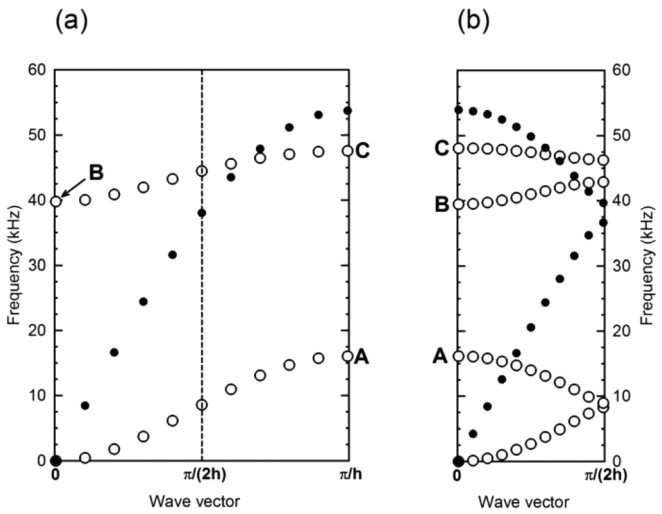

FIG. 4. Band structure of the monoblock (a) and of the diblock (b) Cosserat 1D discrete lattices. Modes "A" and "C" in (a) and (b) correspond to successive Cosserat elements rotating out-of-phase. Oppositely, mode "B" shows successive Cosserat elements rotating in-phase.

IV. APPLICATION OF DIRAC FORMALISM TO ROTATIONAL WAVES

A. Discrete monoblock model of rotational waves

For the sake of simplicity, we restrict this model to the propagation of rotational waves by allowing only rotation of the blocks about their center of mass and by constraining shear and longitudinal displacements in the monoblock lattice. The equation of motion associated with the rotational degrees of freedom (Eq. (4)) then takes the simpler general form

$$I\frac{\partial^2\varphi_n}{\partial t^2} = K_1'(\varphi_{n+1} - 2\varphi_n + \varphi_{n-1}) - K_2'\varphi_n, \quad (5)$$

$K_1' = K_2 - \frac{h^2 K_1}{4}$, and $K_2' = h^2 K_1$. Dividing the equation by I yields our rotational wave equation

$$\frac{\partial^2 \varphi_n}{\partial t^2} - \beta^2(\varphi_{n+1} - 2\varphi_n + \varphi_{n-1}) + \alpha^2 \varphi_n = 0 \qquad (6)$$

with $\beta^2 = \frac{K_1'}{I}$ and $\alpha^2 = \frac{K_2'}{I}$. We will consider three cases. For case I, K_1', and K_2' are taken as positive constants. For case II, $\alpha^2 = 0$ (i.e., $K_2' = 0$). For case III, we take $K_2 = 0$ (i.e., $k_1 = 0$, that is, only harmonic springs between opposite vertices of the blocks are considered). Under this last condition, $K_1' < 0$ and we take $\beta = i\beta'$ ($\beta^2 = -\beta'^2$) and $\alpha = 2\beta'$ ($\alpha^2 = 4\beta'^2$) with $\beta' > 0$. Note that the 1-D system studied numerically in Sec. III falls into the case I of the subsequent Dirac formalism.

B. Dirac equation and solutions for rotational waves

Equation (6) involves the second derivatives with respect to continuous time and the discrete second derivative with respect to position of the angular degree of freedom. Here, following the approach of Dirac in linearizing the relativistic Klein-Gordon equation, we wish to derive a wave equation in terms of first order spatial and temporal derivatives. To do this, we need to rewrite the Laplacian, $\Delta\varphi_n = \varphi_{n+1} - 2\varphi_n + \varphi_{n-1}$, in a "square root" form: $\Delta\varphi_n = D(D\varphi_n)$. This can be done exactly by introducing the following first order differential operator:

$$D = \boldsymbol{e}_1\Delta^+ + \boldsymbol{e}_2\Delta^- = \begin{pmatrix} 0 & 1 \\ 0 & 0 \end{pmatrix}\Delta^+ + \begin{pmatrix} 0 & 0 \\ 1 & 0 \end{pmatrix}\Delta^-. \qquad (7)$$

In Eq. (7), $\Delta^+\varphi_n = \varphi_{n+1} - \varphi_n$ and $\Delta^-\varphi_n = \varphi_n - \varphi_{n-1}$ are the forward and backward finite differences acting now on a two-vector. The 2×2 matrices $\boldsymbol{e}_1$ and $\boldsymbol{e}_2$ satisfy the conditions $\boldsymbol{e}_1\boldsymbol{e}_1 = \boldsymbol{e}_2\boldsymbol{e}_2 = 0$ and $\boldsymbol{e}_1\boldsymbol{e}_2 + \boldsymbol{e}_2\boldsymbol{e}_1 = \boldsymbol{I}$ with $\boldsymbol{I}$ representing the 2×2 identity matrix. This formalism permits the exact and formal definition of the "square root" of the discrete Laplacian.

The Dirac-like equation for rotational waves corresponding to case I then takes the form

$$\left[\boldsymbol{\sigma_x} \otimes \boldsymbol{I}\frac{\partial}{\partial t} + i\beta\boldsymbol{\sigma_y} \otimes \{\boldsymbol{e}_1\Delta^+ + \boldsymbol{e}_2\Delta^-\} \pm i\alpha\boldsymbol{I} \otimes \boldsymbol{I}\right]\psi = 0, \quad (8)$$

where $\boldsymbol{\sigma_x}$ and $\boldsymbol{\sigma_y}$ are the 2×2 Pauli matrices: $\begin{pmatrix} 0 & 1 \\ 1 & 0 \end{pmatrix}$ and $\begin{pmatrix} 0 & -i \\ i & 0 \end{pmatrix}$, respectively. The parameter α plays the role of mass in the relativistic Dirac equation. Applying the outer product $\otimes$ leads to 4×4 matrices and ψ is a four-vector: $\psi = \begin{pmatrix} \psi_{1n} \\ \psi_{2n} \\ \psi_{3n} \\ \psi_{4n} \end{pmatrix}$. This four component representation is the consequence of the discrete nature of the Laplacian. In contrast, with a continuous Laplacian, there is no distinction between forward and backward derivatives and one would only need to use a two component representation. This is the case in the long wavelength limit of Sec. IV C. In this limit, having a two component spinor indicates that there is a coupling between waves propagating in opposite directions (positive or negative) along the chain of blocks. When considering the short wavelength four component spinor solution, the first two components represent propagation of waves in the positive direction and the next two components propagation in the negative direction. The two components for the positive direction and the two components from the negative directions reflect a lifting of degeneracy due to asymmetry of the forward and backward finite different in the discrete Dirac equation. The solution of Eq. (8), namely ψ, is automatically a solution of Eq. (6), i.e., φ but the converse is not true. As will be seen later, the directions of propagation of the wave are expressed separately in the Dirac wave function. The $\pm$ corresponds to choices of the sign of the parameter α (i.e., choice of positive or negative "mass"). Subsequently, we choose the negative value without consequence on the conclusions drawn. Equation (8) becomes

$$\left[\boldsymbol{C}\frac{\partial}{\partial t} + \beta\{\boldsymbol{A}\Delta^+ + \boldsymbol{B}\Delta^-\} - i\alpha\boldsymbol{I}\right]\psi = 0. \qquad (9)$$

$\boldsymbol{C}$, $\boldsymbol{A}$, $\boldsymbol{B}$, and $\boldsymbol{I}$ are the 4×4 matrices

$$\begin{pmatrix} 0 & 0 & 1 & 0 \\ 0 & 0 & 0 & 1 \\ 1 & 0 & 0 & 0 \\ 0 & 1 & 0 & 0 \end{pmatrix}, \begin{pmatrix} 0 & 0 & 0 & 1 \\ 0 & 0 & 0 & 0 \\ 0 & -1 & 0 & 0 \\ 0 & 0 & 0 & 0 \end{pmatrix}, \begin{pmatrix} 0 & 0 & 0 & 0 \\ 0 & 0 & 1 & 0 \\ 0 & 0 & 0 & 0 \\ -1 & 0 & 0 & 0 \end{pmatrix}, \begin{pmatrix} 1 & 0 & 0 & 0 \\ 0 & 1 & 0 & 0 \\ 0 & 0 & 1 & 0 \\ 0 & 0 & 0 & 1 \end{pmatrix}.$$

It is easily verifiable that $CC = I$, $AA = BB = 0$, $AB + BA = -I$, and $C(A\Delta^+ + B\Delta^-) + (A\Delta^+ + B\Delta^-)C = 0$, which are the conditions necessary to recover the wave Eq. (6) by applying the operator in Eq. (9) twice (with appropriate $\pm$ sign). Equation (9) is the basis for our discussion of fermion-like excitations in phononic structures.

Seeking solutions in the form of plane waves, $\psi_{jn} = a_j e^{-i\omega t}e^{iknh}$ with $j = 1, 2, 3, 4$. ω and k are the angular frequency and wave number, respectively. We remind the reader that "h" is the spacing distance between blocks. Equation (9) yields the system of equations

$$\begin{cases} -i\alpha a_1 - i\omega a_3 + \beta(e^{ikh} - 1)a_4 = 0 \\ -i\alpha a_2 + \beta(1 - e^{-ikh})a_3 - i\omega a_4 = 0 \\ -i\omega a_1 - \beta(e^{ikh} - 1)a_2 - i\alpha a_3 = 0 \\ -\beta(1 - e^{-ikh})a_1 - i\omega a_2 - i\alpha a_4 = 0. \end{cases} \qquad (10)$$

This system of equation admits two doubly degenerate Eigen values

$$\omega = \pm\sqrt{\alpha^2 - \beta^2(e^{ikh}-1)(1-e^{-ikh})} = \pm\sqrt{\alpha^2 + 4\beta^2\sin^2\frac{kh}{2}}. \quad (11)$$

The negative frequency can be interpreted physically as follows.[28] Since the angular field ought to be a real-valued quantity, it can be written as the sum of a complex term and its complex conjugate. The negative frequency is associated with the complex conjugate term.

The rotational mode at the origin, k = 0, has a finite frequency and is isomorphic to mode "B" observed in the 2D and 1D phononic structures.

We note that Eq. (11) gives two branches with positive and negative frequencies that do not intersect at the origin unless $\alpha = 0$. The dispersion relations are periodic and defined in the first Brillouin zone: $k \in \left[-\frac{\pi}{h}, \frac{\pi}{h}\right]$. Choosing the positive or negative branches of the dispersion relations, we determine the four Eigen vectors for case I

$$\begin{pmatrix} a_1 \\ a_2 \\ a_3 \\ a_4 \end{pmatrix} = a_0 \begin{pmatrix} -e^{i\frac{kh}{4}}\sqrt{\alpha-\beta(e^{i\frac{kh}{2}}-e^{-i\frac{kh}{2}})} \\ -\mp ie^{-i\frac{kh}{4}}\sqrt{\alpha+\beta(e^{i\frac{kh}{2}}-e^{-i\frac{kh}{2}})} \\ \pm e^{i\frac{kh}{4}}\sqrt{\alpha+\beta(e^{i\frac{kh}{2}}-e^{-i\frac{kh}{2}})} \\ +ie^{-i\frac{kh}{4}}\sqrt{\alpha-\beta(e^{i\frac{kh}{2}}-e^{-i\frac{kh}{2}})} \end{pmatrix}. \quad (12a)$$

$$\begin{pmatrix} a_1 \\ a_2 \\ a_3 \\ a_4 \end{pmatrix} = a_0 \begin{pmatrix} -e^{i\frac{kh}{4}}\sqrt{\alpha+\beta(e^{i\frac{kh}{2}}-e^{-i\frac{kh}{2}})} \\ +ie^{-i\frac{kh}{4}}\sqrt{\alpha-\beta(e^{i\frac{kh}{2}}-e^{-i\frac{kh}{2}})} \\ +e^{i\frac{kh}{4}}\sqrt{\alpha-\beta(e^{i\frac{kh}{2}}-e^{-i\frac{kh}{2}})} \\ -ie^{-i\frac{kh}{4}}\sqrt{\alpha+\beta(e^{i\frac{kh}{2}}-e^{-i\frac{kh}{2}})} \end{pmatrix}. \quad (12b)$$

The upper signs in Eqs. (12a) and (12b) correspond to the positive branch of the wave function and the lower signs to the negative branch. The Eigen vectors given by Eqs. (12) have the characteristic property of being 4π periodic in k, which is often associated with spinors. In Sec. IV C, we investigate several limits of the Eqs. (9) and (10) and Eigen values and Eigen vectors given by Eqs. (11) and (12).

In the limit $\alpha \to 0$ (case II), Eq. (11) reduces to the well-known dispersion relation for the one-dimensional harmonic chain.

C. Long wavelength limit and related systems

In the long wavelength limit, $k \to 0$, the system of Eq. (10) reduces to first order to

$$\begin{cases} \alpha a_1 + \omega a_3 - \beta kh a_4 = 0 \\ \alpha a_2 - \beta kh a_3 + \omega a_4 = 0 \\ \omega a_1 + \beta kh a_2 + \alpha a_3 = 0 \\ \beta kh a_1 + \omega a_2 + \alpha a_4 = 0, \end{cases} \quad (13)$$

where $\alpha = \sqrt{\omega^2 - (\beta kh)^2}$. By setting $a_1 = a_2 = a_1'$ and $a_3 = a_4 = a_2'$, we obtain the reduced system of two linear equations

$$\begin{cases} \alpha a_1' = -(\omega - \beta kh)a_2' \\ (\omega + \beta kh)a_1' = -\alpha a_2'. \end{cases} \quad (14)$$

We could have obtained the same reduction in order of the system of equation by adding the first two equations in the system of Eqs. (13) and the last two equations and setting $a_1' = a_1 + a_2$ and $a_2' = a_3 + a_4$. This reduction from a fourth order to a second order system of linear equations reflects the fact that in the long wavelength limit the difference between forward and backward finite differences is lost. The difference between the sublattices supporting the two types of spatial finite differences is lost in the continuum limit. The four-spinor reduces to a two-spinor, $\begin{pmatrix} a_1' \\ a_2' \end{pmatrix}$, which would be solutions of the continuous wave equation

$$\left[\boldsymbol{\sigma_x}\frac{\partial}{\partial t} + i\beta\boldsymbol{\sigma_y}\frac{\partial}{\partial x} \pm i\alpha\boldsymbol{I}\right]\psi = 0. \quad (15)$$

The Eigen values are given by $\omega = \pm\sqrt{\alpha^2 + \beta^2(kh)^2}$ and the two-spinor corresponding to the positive branch takes the form

$$\begin{pmatrix} a_1' \\ a_2' \end{pmatrix} = a_0 \begin{pmatrix} -\sqrt{\omega - \beta kh} \\ +\sqrt{\omega + \beta kh} \end{pmatrix}. \quad (16)$$

We also note that if $\alpha = 0$ (case II), the system of Eq. (14) reduces to $\begin{cases} (\omega - \beta kh)a_1' = 0 \\ (\omega + \beta kh)a_2' = 0 \end{cases}$. These are Eigen values solutions of the continuous wave equation

$$\left[\boldsymbol{\sigma_x}\frac{\partial}{\partial t} + i\beta\boldsymbol{\sigma_y}\frac{\partial}{\partial x}\right]\psi = 0. \quad (17)$$

We obtain two solutions for the angular velocity of the plane wave, $\omega = \pm\beta kh$. These correspond to plane waves propagating in the positive and negative directions. In case II, the components of the two-spinor, a_1' and a_2', are now independent of each other, which is the amplitude of the plane wave propagating in the positive direction (positive frequency) is independent of that of the wave propagating in the opposite sense (negative frequency). By opposite sense, we mean waves propagating along different directions. When $\alpha \neq 0$, from Eq. (16), we see that the components of the two-spinor, a_1' and a_2', are not independent of each other. This indicates that the senses of propagation of a wave (positive or negative) are not independent of each other. It is the parameter α that couples those senses. The quantity α leads to a coupling between the components (sense of wave). Equation (6) is isomorphic to the equation of propagation of waves in a one-dimensional discrete harmonic chain with a distribution of scattering centers on each site of the chain.[1] Each scattering center is associated with a perturbation: $V = \alpha$. It is well

known that if one considers a 1-D harmonic chain with a single local perturbation, an incident wave propagating in the positive direction will be scattered into a transmitted wave and a reflected wave. The reflected wave is now propagating in the negative direction and its amplitude is related to that of the incident wave through the reflection coefficient. In the system described by Eq. (6), multiple scattering at every site results in the coupling between the senses of propagation of the waves.

Taking the limit $\alpha \to 0$ (case II) in Eq. (12a), the four-spinor solution for the positive branch of the band structure becomes

$$\begin{pmatrix} a_1 \\ a_2 \\ a_3 \\ a_4 \end{pmatrix} = a_0 \begin{pmatrix} -ie^{i\frac{kh}{4}}\sqrt{\beta\left(e^{i\frac{kh}{2}} - e^{-i\frac{kh}{2}}\right)} \\ -ie^{-i\frac{kh}{4}}\sqrt{\beta\left(e^{i\frac{kh}{2}} - e^{-i\frac{kh}{2}}\right)} \\ e^{i\frac{kh}{4}}\sqrt{\beta\left(e^{i\frac{kh}{2}} - e^{-i\frac{kh}{2}}\right)} \\ -e^{-i\frac{kh}{4}}\sqrt{\beta\left(e^{i\frac{kh}{2}} - e^{-i\frac{kh}{2}}\right)} \end{pmatrix} = a_0'(k) \begin{pmatrix} e^{i\frac{\pi}{2}} \begin{pmatrix} e^{i\frac{kh}{4}} \\ e^{-i\frac{kh}{4}} \end{pmatrix} \\ \begin{pmatrix} -e^{i\frac{kh}{4}} \\ e^{-i\frac{kh}{4}} \end{pmatrix} \end{pmatrix}. \tag{18}$$

In Eq. (18), we have separated the four components of the spinor into two groups that correspond to the "positive" and "negative" wave senses. This is still a four-spinor due to the discrete nature of the system and the differentiation between forward and backward finite differences (i.e., due to the two sublattices on which the finite differences are defined). We also note that the first group (positive sense) is $\frac{\pi}{2}$ out of phase with the second group (negative sense). It is only in the long wavelength limit that the two senses become independent. For instance, we can reduce the four-spinor in Eq. (18) to the form of a two spinor: $\begin{pmatrix} e^{i\frac{\pi}{2}}\left(e^{i\frac{kh}{4}} + e^{-i\frac{kh}{4}}\right) \\ \left(-e^{i\frac{kh}{4}} + e^{-i\frac{kh}{4}}\right) \end{pmatrix}$, which in the long wavelength limit reduces to $\begin{pmatrix} 2e^{i\frac{\pi}{2}} \\ 0 \end{pmatrix}$. Note that Eq. (18) was obtained in the case of the positive branch of the dispersion relations. When considering the negative branch, one finds the following for the reduce two-spinor in the long wavelength limit: $\begin{pmatrix} 0 \\ 2 \end{pmatrix}$. The positive sense is decoupled from the negative sense. It is worth noting that even though in the long wavelength limit senses are decoupled, they are still $\frac{\pi}{2}$ out of phase. Such an observation could not be made by solving Eq. (17) directly. This observation originates from the sublattice dependent spatial finite differences of the discrete equations. Similar observations are made for all the Eigen vectors given by Eqs. (12a) and (12b).

In case III, the Eigen values are obtained as positive and negative dispersion relations $\omega = \pm\sqrt{4\beta'^2\cos^2\left(\frac{kh}{2}\right)}$ and the four-spinor of Eq. (12a) reduces to

$$\begin{pmatrix} a_1 \\ a_2 \\ a_3 \\ a_4 \end{pmatrix} = a_0\sqrt{2\beta'} \begin{pmatrix} \begin{matrix} - \\ - \end{matrix} e^{i\frac{kh}{4}}\sqrt{1 + \sin\left(\frac{kh}{2}\right)} \\ \mp ie^{-i\frac{kh}{4}}\sqrt{1 - \sin\left(\frac{kh}{2}\right)} \\ \pm e^{i\frac{kh}{4}}\sqrt{1 - \sin\left(\frac{kh}{2}\right)} \\ \begin{matrix} + \\ + \end{matrix} ie^{-i\frac{kh}{4}}\sqrt{1 + \sin\left(\frac{kh}{2}\right)} \end{pmatrix} \tag{19a}$$

$$\begin{pmatrix} a_1 \\ a_2 \\ a_3 \\ a_4 \end{pmatrix} = a_0\sqrt{2\beta'} \begin{pmatrix} \begin{matrix} - \\ + \end{matrix} e^{i\frac{kh}{4}}\sqrt{1 - \sin\left(\frac{kh}{2}\right)} \\ \begin{matrix} + \\ + \end{matrix} ie^{-i\frac{kh}{4}}\sqrt{1 + \sin\left(\frac{kh}{2}\right)} \\ \begin{matrix} + \\ + \end{matrix} e^{i\frac{kh}{4}}\sqrt{1 + \sin\left(\frac{kh}{2}\right)} \\ \begin{matrix} - \\ + \end{matrix} ie^{-i\frac{kh}{4}}\sqrt{1 - \sin\left(\frac{kh}{2}\right)} \end{pmatrix}. \tag{19b}$$

Again in Eqs. (19a) and (19b), the upper and lower signs refer to the positive and negative dispersion relations.

D. Constraints on wave functions

We have determined that when linearizing the wave equation for rotational waves, the solutions have spinor character. The spinor character is associated with the separation of the sense of propagation of waves along the one-dimensional axis of our system. In addition, in the case of the discrete one-dimensional system, the separation of the spatial derivative operator into direction (sublattice) sensitive finite differences introduces a possible phase shift between the two senses of propagation. In this section, we explore the consequence of the phase difference between spinor components (wave sense) and band structure.

We first write the wave function solution of the Dirac-like equation in the general form $\psi(\omega,k) = \xi(k)\phi(\omega,k)$, where $\xi(k)$ is the spinor part and $\phi(\omega,k)$ is the spatio-temporal part of the wave function. For continuous systems, $\phi(\omega,k) = e^{-i\omega t}e^{ikx}$; and for discrete systems, $\phi(\omega,k) = e^{-i\omega t}e^{iknh}$. We consider some Hermitian operator, Q, corresponding to some observable that acts only on the spinor part of the wave function, then: $\psi^*Q\psi = \xi^*\phi^*Q\xi\phi = (\xi^*Q\xi)\phi^*\phi$. Let us now treat the case of the linear superposition of two wave functions, $\psi = \psi_A + \psi_B$ with $\psi_A(\omega_A,k_A)$ and $\psi_B(\omega_B,k_B)$. The observable for the superposition of the two waves takes the form

$$\begin{aligned}\psi^*Q\psi = &\left(\xi_A^*Q\xi_A\right)\phi_A^*\phi_A + \left(\xi_B^*Q\xi_B\right)\phi_B^*\phi_B \\ &+ \left(\xi_A^*Q\xi_B\right)\phi_A^*\phi_B + \left(\xi_B^*Q\xi_A\right)\phi_B^*\phi_A.\end{aligned} \tag{20}$$

The first two terms are the observables for each wave. The last two terms correspond to interference terms that should add to zero for an additive operator Q (i.e., an operator for

which the observable for a superposition of states is the sum of the observables of individual states).

We will explore initially superpositions of two waves with the same wave vector $k_A = k_B = k$ as well as assuming that the two solutions belong to the same positive branch of the dispersion relation. Since we have seen that the spinor components of the wave function for the three cases I, II, and III depend on k only, we can rewrite the Eq. (20) as

$$\psi^* Q \psi = (\xi^* Q \xi)\phi_A^* \phi_A + (\xi^* Q \xi)\phi_B^* \phi_B + (\xi^* Q \xi)\{\phi_A^* \phi_B + \phi_B^* \phi_A\}. \quad (21)$$

Finally since the functions ϕ are extended over time and space, we calculate the observable by integrating Eq. (21) over these variables. Provided that the observables of the operator Q are non-zero (i.e., $\xi^* Q \xi \neq 0$), then the additive property of the observables leads to the following condition on the integral of the spatio-temporal part of the wave function:

$$\int\int (\phi_A^* \phi_B + \phi_B^* \phi_A) dt dx = \int\int (e^{i(\omega_A - \omega_B)t} + e^{-i(\omega_A - \omega_B)t}) dt dx = 2\int dx \int dt \cos(\omega_A - \omega_B)t = 0. \quad (22)$$

Such a condition is possible only if $\omega_A \neq \omega_B$. Therefore, when there exists a Hermitian operator that operates on the spinor-part of the wave function with a value for the corresponding observable different from zero, then the integral of the spatio-temporal part of the wave function is equal to zero. This means that for the same value of k, the frequency is non-degenerate and the band structure should possess two non-degenerate branches. Otherwise, if the spinor-related observables are zero, there is no constraint on the integral of the spatio-temporal part of the wave function. The band structure may possess degenerate points where two branches cross at the same frequency.

We use the operator Q given by the 4×4 matrix: $\boldsymbol{C} = \boldsymbol{\sigma_x} \otimes \boldsymbol{I}$ that acts only on the spinor part of the wave function. For case I, using the four-spinor given by Eq. (12a), we get $\xi^* Q \xi = -4a_0^2 \alpha$. Since this quantity is different from zero, then for all wave number, k, there cannot be any degenerate points in frequency within the Brillouin zone.

In the limit $\alpha \to 0$, corresponding to case II, the quantity $\xi^* Q \xi = 0$ for all wave numbers. This indicates that the spinor part of the wave function does not impose any constraint on the integral of the spatio-temporal part of the wave function. Degenerate and non-degenerate branches are possible in the band structure but non-degeneracy is not imposed by the spinor characteristics of the wave function. In the last case, namely case III, $\xi^* Q \xi = -8a_0^2 \beta' \sqrt{\cos^2(\frac{hk}{2})}$. This observable is non-zero for all wave numbers $k \in [0, \frac{\pi}{h}]$. The band structure does not show any degenerate point as imposed by the spinor part of the wave function. At the edge of the Brillouin zone, $k = \frac{\pi}{h}$, $\xi^* Q \xi = 0$, which indicates that there could exist a degenerate point at that location. This is indeed the case.

We now explore superpositions of two waves with the same wave vector $k_A = k_B = k$ but corresponding to the positive and the negative branches of the dispersion relation.

In case I, we find $\xi_A^* Q \xi_B = -\xi_B^* Q \xi_A = -ia_0^2 8\beta \sin \frac{kh}{2}$. These quantities are different from zero for $k \neq 0$. The interference terms in Eq. (20) will then add to zero when $\int\int (\phi_A^* \phi_B - \phi_B^* \phi_A) dt dx = 0$. This condition is always satisfied since we have chosen $\omega_A = -\omega_B = \omega$. At $k = 0$, the spinor part of the wave function does not impose constraints on the integral of the spatio-temporal part. We need to keep in mind that here those two wave functions have $\omega_A = -\omega_B = \omega$.

When $k_A = k_B = k$ and $\omega_A = -\omega_B = \omega$, case II similarly to case I does not lead to any constraints on the spatio-temporal part of the wave function. Finally, for case III, we determine: $\xi_A^* Q \xi_B = \xi_B^* Q \xi_A = 0$, which leads to the same conclusions as the other two cases. These results are completely consistent with those found when we assume $k_A = k_B = k$ and two superposed waves with frequency from the same positive branch.

In summary, the degeneracy of bands at a given wave number, k, depends on the spinor part of the wave function. In the case of rotational waves corresponding to cases I and III, the spinor part of the wave function does indeed constrain the integral of the spatio-temporal part of the wave function leading to non-degenerate Eigen values for all (case I) or most (case III) wave numbers. In the case II of the usual 1D wave equation ($\alpha = 0$), the spinor part of the wave equation imposes no constraint on the integral of the spatio-temporal part. In this last case, degeneracy or non-degeneracy of the band structure is unrelated to the spinor part of the wave function.

It is important to recall that the third band in the band structure of the monoblock lattice corresponds to the band analyzed analytically in this section. Mode "B" where blocks rotate in phase corresponds to the long wavelength limit of that band. In particular, this band corresponds to the rotational waves of case I and/or III. We have just shown that, at this point, degeneracy of rotational modes (i.e., $\omega = -\omega = 0$) is forbidden due to the characteristics of the spinor part of the wave function. The fact that this rotational mode is occurring with a non-zero frequency at the Γ point is indicative of a mode that has spinor structure and therefore of dispersion relation that results from fermion-like behavior.

V. CONCLUSIONS

We have analyzed computationally a 2D phononic crystal composed of a square array of cylindrical inclusion (square cross section) of PS embedded in a soft elastomeric matrix of PDMS. The calculated band structure of this system, along the ΓM direction of the Brillouin zone, possesses several branches that support waves with rotational degrees of freedom. In particular, we identify a band that has a non-zero frequency at the Γ point. Analysis of this mode indicates that this is a pure rotational mode where the PS inclusions and the PDMS regions separating the inclusions undergo rotational oscillations in phase. This mode is identified to correspond to the fermion-like mode studied using a

1D discrete block-spring model. First, the 1D model is used to reproduce the dispersion relations of the 2D system in a certain range. This 1D discrete Cosserat-type block-spring model is then analyzed within the Dirac's formalism. We have shown that rotational waves are characterized by wave functions that include a spinor part and a spatio-temporal part. The spinor part is related to the coupling between the senses of wave propagation. The spatio-temporal part of the wave function retains its plane-wave character. By calculating observables associated with operators that operate only on the spinor part of the wave function, for the superposition of two waves, we have identified conditions that constrain Eigen states of the system. In particular, we have identified conditions that impose the lifting of the frequency degeneracy at the origin of the Brillouin zone. This observation suggests that rotational modes in PC may possess fermion-like (or spinor-related) characteristics, which effects can be observed in their band structure. As mentioned before, the spinor-part of the rotational wave functions reflects a coupling between positive and negative sense for the propagation of the wave. The fermion-like behavior that we characterized lifts the degeneracy between bands with positive negative frequency at the origin of the Brillouin zone.

From a practical point of view, the fermion-like behavior we report can also be observed in phononic crystals composed of a square array of cylindrical inclusions with circular cross sections. Furthermore, the observation of the in-phase rotational mode at low frequency is made possible by the very low transverse speed of sound of the elastomer matrix. This type of rotational mode would still exist for a composite material with a stiffer matrix but would then appear at higher frequency. At higher frequency, the in-phase rotational mode would most probably interact with numerous other modes rendering its analysis a lot more complex than in the case of a soft matrix material.

It might be useful to be able to detect wave propagation sense to shed light on the sense-related characteristics of waves. Non-linear wave phenomena would appear to provide such means. To that effect, we would like to cite the work of Rubino *et al.*[28] who have been able to observe the coupling of an optical soliton wave to the negative frequency branch of the optical dispersion relation of bulk CaF_2 crystal and fused silica-optical fiber. Further, we have shown recently in a molecular dynamics simulation of a non-linear 1D monoatomic crystal the emergence at the edge of the Brillouin zone of non-linear satellite modes nearly symmetrical about the frequency-shifted linear mode. The satellite peaks are due to the wave-number conserving interaction between a short wavelength "test" wave with positive frequency and long wavelength modes belonging to both the positive and negative branches of the dispersion relation.[27]

Furthermore, PC supporting translational waves have been demonstrated to possess a plethora of functions resulting from unique features in their band structures, namely spectral properties (stop bands, passing bands, frequency filtering, etc.) or wave number properties (negative refraction, zero angle refraction, superlensing, etc.).[1] The fermion-like behavior of some rotational waves characterized in this paper opens up opportunities in the control of the direction of propagation of elastic waves. For instance, we have seen in the long wavelength limit that the two spinor solution represents coupling between wave propagating in opposite directions. The spinor part of the wave function can be projected on the orthonormal basis $\begin{pmatrix}1\\0\end{pmatrix}$ and $\begin{pmatrix}0\\1\end{pmatrix}$ representing the possible directions of propagation of the wave. This enables us to encode information in the relative weight (phase) of the directions of propagation by controlling the wavenumber, k. Applications in information processing would emerge from this control.

Finally, the present study was limited to linear 2D and 1D PC models supporting rotational waves. However, rotational degrees of freedom should lead to geometric non-linearity. The non-linearity of rotational waves is anticipated to result in unique functionalities. From a practical point of view, one can excite rotational modes by stimulating the PC with transverse waves as shear and rotational modes are coupled, thus enabling the potential development of rotational wave-based phononic devices.

[1]*Acoustic Metamaterials and Phononic Crystals*, Springer Series in Solid State Sciences, editor by P. A. Deymier (Springer, Heidelberg, 2013), p. 173.
[2]F. Liu, Y. Lai, X. Huang, and C. T. Chan, Phys. Rev. B **84**, 224113 (2011).
[3]G. Wang, X. Wen, J. Wen, L. Shao, and Y. Liu, Phys. Rev. Lett. **93**, 154302 (2004).
[4]Y. Lai, Y. Wu, P. Sheng, and Z. Q. Zhang, Nature Mater. **10**, 620 (2011).
[5]R. Sainidou, N. Stefanou, and A. Modinos, Phys. Rev. B **66**, 212301 (2002).
[6]H. Zhao, Y. Liu, G. Wang, J. Wen, D. Yu, X. Han, and X. Wen, Phys. Rev. B **72**, 012301 (2005).
[7]K. Maslov, V. K. Kinra, and B. K. Henderson, Mech. Mater. **31**, 175 (1999).
[8]P. Peng, J. Mei, and Y. Wu, Phys. Rev. B **86**, 134304 (2012).
[9]E. Cosserat and F. Cosserat, *Théorie des Corps Déformables* (Hermann et Fils, Paris, 1909).
[10]R. Lakes, in *Continuum Models for Materials with Microstructure*, edited by H. Muhlhaus (John Wiley and Sons, New York, 1995).
[11]A. Merkel, V. Tournat, and V. Gusev, Phys. Rev E **82**, 031305 (2010).
[12]V. Tournat, I. Pérez-Arjona, A. Merkel, V. Sanchez-Morcillo, and V. Gusev, New J. Phys. **13**, 073042 (2011).
[13]A. Merkel, V. Tournat, and V. Gusev, Phys. Rev. Lett. **107**, 225502 (2011).
[14]J. Burnett and D. Vassiliev, Mathematika **58**, 349 (2012).
[15]R. A. Close, Adv. Appl. Clifford Algebras **21**, 273 (2011).
[16]C. T. Chan, Z. H. Hang, and X. Huang, Adv. Optoelectron. **2012**, 313984.
[17]J. M. Zeuner, N. K. Efremedis, R. Keil, F. Dreisow, D. N. Christodoulis, A. Tunnermann, S. Nolte, and A. Szameit, Phys. Rev. Lett **109**, 023602 (2012).
[18]V. Mocella, S. Cabrini, A. S. P. Chang, P. Dardano, L. Moretti, I. Rendina, D. Olynick, B. Harteneck, and S. Dhuey, Phys. Rev. Lett. **102**, 133902 (2009).
[19]O. Peleg, G. Bartal, B. Freedman, O. Manela, M. Segev, and D. N. Christodoulides, Phys. Rev. Lett. **98**, 103901 (2007).
[20]F. Liu, X. Huang, and C. T. Chan, Appl. Phys. Lett. **100**, 071911 (2012).
[21]J. Mei, Y. Wu, C. T. Chan, and Z.-Q. Zhang, Phys. Rev. B **86**, 035141 (2012).
[22]S. Longhi, Opt. Lett. **35**, 235 (2010).
[23]S. Longhi, Opt. Lett. **35**, 1302 (2010).
[24]P. A. M. Dirac, Proc. R. Soc. A **117**, 610 (1928).
[25]A. Vasiliev, A. Miroshnichenko, and M. Ruzzene, Mech. Res. Commun. **37**, 225–229 (2010).
[26]A. Vasiliev, A. Miroshnichenko, and M. Ruzzene, J. Mech. Mater. Struct. **3**, 1365–1382 (2008).
[27]N. Swinteck, K. Muralidharan, and P. A. Deymier, J. Vib. Acoust. **135**, 041016 (2013).
[28]E. Rubino, J. McLenaghan, S. C. Kehr, F. Belgiorno, D. Townsend, S. Rohr, C. E. Kuklewicz, U. Leonhardt, F. Konig, and D. Faccio, Phys. Rev. Lett. **108**, 253901 (2012).